Original Article
BMP4 augments the survival of hepatocellular carcinoma (HCC) cells under hypoxia and hypoglycemia conditions by promoting the glycolysis pathway

Jiamin Zhong[1], Quan Kang[2], Youde Cao[3], Baicheng He[4], Piao Zhao[1], Yannian Gou[1], Yetao Luo[5], Tong-Chuan He[6], Jiaming Fan[1]

[1]Ministry of Education Key Laboratory of Diagnostic Medicine, Department of Clinical Biochemistry, College of Laboratory Medicine, Chongqing Medical University, Chongqing 400016, China; [2]Stem Cell Biology and Therapy Laboratory, Ministry of Education Key Laboratory of Child Development and Disorders, The Children's Hospital of Chongqing Medical University, Chongqing 400014, China; [3]Department of Pathology, Chongqing Medical University, Chongqing 400016, China; [4]Department of Pharmacology, School of Pharmacy, Chongqing Medical University, Chongqing 400016, China; [5]Clinical Epidemiology and Biostatistics Department, Department of Pediatric Research Institute, Children's Hospital of Chongqing Medical University, Chongqing 400014, China; [6]Molecular Oncology Laboratory, Department of Orthopaedic Surgery and Rehabilitation Medicine, The University of Chicago Medical Center, Chicago, IL 60637, USA

Abstract: Hepatocellular carcinoma (HCC) is one of the leading causes of cancer death worldwide although its pathogenic mechanism remains to be fully understood. Unlike normal cells, most cancer cells rely on aerobic glycolysis and are more adaptable to the microenvironment of hypoxia and hypoglycemia. Bone Morphogenetic Protein 4 (BMP4) plays important roles in regulating proliferation, differentiation, invasion and migration of HCC cells. We have recently shown that BMP4 plays an important role in regulating glucose metabolism although the effect of BMP4 on glucose metabolic reprogramming of HCC is poorly understood. In this study, we found that BMP4 was highly expressed in HCC tumor tissues, as well as HCC cell lines that were tolerant to hypoxia and hypoglycemia. Mechanistically, we demonstrated that BMP4 protected HCC cells from hypoxia and hypoglycemia by promoting glycolysis since BMP4 up-regulated glucose uptake, the lactic acid production, the ATP level, and the activities of rate limiting enzymes of glycolysis (including HK2, PFK and PK). Furthermore, we demonstrated that BMP4 up-regulated HK2, PFKFB3 and PKM2 through the canonical Smad signal pathway as SMAD5 directly bound to the promoter of PKM. Collectively, our findings shown that BMP4 may play an important role in regulating glycolysis of HCC cells under hypoxia and hypoglycemia condition, indicating that novel therapeutics may be developed to target BMP4-regulated glucose metabolic reprogramming in HCC.

Keywords: BMP4, HCC, hypoxic and hypoglycemic, glycolysis, metabolic reprogramming, Smad signal pathway

Introduction

HCC is one of the leading causes of cancer death worldwide, and its incidence has been increasing in the last decade although its molecular pathogenesis remains to be fully understood [1]. Since the liver is an important organ of human in regulating glucose homeostasis and lipid metabolism, the changes of energy metabolism in liver cancer cells cannot been ignored [2, 3]. One of the best characterized metabolic phenotypes observed in tumor cells is the phenomenon termed "the Warburg effect" [2, 4, 5]. In contrast to normal cells, which mainly rely on mitochondrial oxidative phosphorylation to generate the energy, most cancer cells instead rely on aerobic glycolysis needed for cellular processes [2, 5, 6]. Rapidly growing tumors invariably contain hypoxic regions. Adaptive response to hypoxia through angiogenesis, enhanced glucose metabolism and diminished but optimized mitochondrial respiration provides survival and growth advantage to hypoxic tumor cells [7]. This abnormal

glycolysis of tumor cells is thus usually accompanied with increased glucose uptake and lactic acid production, which is conducive to the occurrence and development of tumor [7].

Bone morphogenetic proteins (BMPs) belong to the transforming growth factor β (TGF-β) superfamily, and play important roles in regulating embryonic development, stem cell differentiation, and adult tissue homeostasis [8-13]. There are at least 14 types of BMPs in rodents and humans. BMP4 is highly expressed in the liver and plays multiple roles in the proliferation, invasion, migration and differentiation of HCC [14-17]. BMP4 preferentially binds to cytoplasm membrane receptor BMPR-II (type-II receptors), ALK-3 and/or ALK-6 (type-I receptors), and activates receptor-regulated Smads (R-Smads) Smad1, 5 and 8 located in the cytoplasm through phosphorylation activated by type-I receptors. The phosphorylated R-Smads interact with common-partner Smad (co-Smad) Smad4 to form Smad complex, which is then translocated into the nucleus to interact with specific transcription factors and regulate the expression of target genes [9, 10, 18]. Inhibitor Smad6 preferentially inhibits Smad signaling initiated by ALK-3 and ALK-6, whereas inhibitor Smad7 inhibits both TGF-β and Smad signaling [19]. It was shown that BMP4, among the 14 types of BMPs, played an important role in regulating glucose metabolism, and BMP4-BMPR1A signaling in β cells was required for and augmented glucose-stimulated insulin secretion [20]. It was reported that inhibition of BMP4 restored endothelial function in db/db diabetic mice [21]. Nonetheless, the direct impact of BMP4 on glucose metabolic reprogramming in HCC remains poorly understood.

In this study, we sought to investigate the effects and mechanism of BMP4 on HCC cell survival in the microenvironment of hypoxia and hypoglycemia from the view of glycolysis. We found that BMP4 was highly expressed in HCC tumor tissues, as well as HCC cell lines that were tolerant to hypoxia and hypoglycemia. Mechanistically, we demonstrated that BMP4 protected HCC cells from hypoxia and hypoglycemia by promoting glycolysis through a direct regulation of the rate limiting enzymes of glycolysis via the canonical Smad signal pathway. Thus, our findings strongly suggest that BMP4 may play an essential role in regulating glycoly-

sis of HCC cells under hypoxia and hypoglycemia condition, indicating that novel therapeutics may be developed to target BMP4-regulated glucose metabolic reprogramming in HCC.

Materials and methods

The use of human/clinical samples

In this study, we isolated primary human hepatocytes from the surgically resected liver tissues from pediatric patients suffering from cholangiectasis, operated at the Children's Hospital Affiliated to Chongqing Medical University. Furthermore, 40 cases of achieved HCC tissue blocks from the Department of Pathology of Chongqing Medical University were selected for immunohistochemical (IHC) analysis. The use of the clinical samples was approved by the Research Ethics and Regulations Committee of Chongqing Medical University, Chongqing, China.

Cell culture and chemicals

293pTP and RAPA cells were previously described [22, 23]. Human HCC lines Hu7 and MHCC97H cells were provided by the Ministry of Education Key Laboratory of Diagnostic Medicine of Chongqing Medical University. Human primary hepatocytes (HPH) cells were isolated from the human liver tissues which surgically resected from the children with cholangiectasis. All cells were maintained in high glucose DMEM supplemented with 10% FBS (Lonsa Science SRL), 100 units of penicillin and 100 μg of streptomycin at 37°C in 5% CO_2.

For the hypoxia and hypoglycemia culture conditions, cells were maintained in low glucose DMEM and hypoxia was chemically induced by cobalt chloride (100 μM $CoCl_2$) as described [24, 25]. All chemicals were purchased from Sigma-Aldrich (St Louis, MO, USA), Thermo Fisher Scientific (Waltham, MA, USA), or Solarbio (Beijing, China).

H&E and Immunohistochemical (IHC) staining

The paraffin sections of liver tumor tissue (T) and adjacent liver non-tumor tissue (ALNT) samples from 40 HCC patients were obtained from the Department of Pathology of Chongqing Medical University. H&E and IHC staining were conducted following the procedure as

described [26-28]. The antibodies against BMP4 (1:200 dilution; Proteintech; Cat# 12492-1-AP), HK2 (1:200 dilution; Proteintech; Cat# 22029-1-AP), PFKFB3 (1:50 dilution; Bimake; Cat# A5593), PKM2 (1:50 dilution; Bimake; Cat# A5356), SMAD5 (1:50 dilution; Bimake; Cat# A5511) and p-SMAD5 phospho S463 + S465 (1:200 dilution; Abcam; Cat# ab92698). Control rabbit IgG (1:200; cat. no. 011-000-003; Jackson Immuno Research Laboratories, Inc.). The scoring standard and criteria of HCC tissue and adjacent liver non-tumor tissue samples for anti-BMP4 IHC were shown in Table S1 [29].

Construction and amplification of recombinant adenoviruses

Recombinant adenoviruses were generated by using the AdEasy technology [30]. The Ad-B4 that overexpresses human BMP4 was generated as described in previous studies [31, 32]. Ad-siB4 that silence human *Bmp4* was generated as described [33-37]. Three siRNA sites targeting human *BMP4* were shown in Table S2. Adenoviral vector expresses RFP (Ad-RFP) or GFP (Ad-GFP) was used as a control [38, 39].

Crystal violet cell viability assay

Crystal violet staining assay was conducted as described [40, 41]. Briefly, cells were seeded into a 24-well plate at the density of 3×10^4/well and treated by different conditions. At the indicated time points, the cells were stained with 0.5% crystal violet/formalin solution. For quantitative measurement, the stained cells were dissolved in 10% acetic acid, followed by measuring absorbance at 592 nm.

WST-1 cell proliferation assay

WST-1 assay was conducted as described [40, 41]. Briefly, cells were seeded into a 96-well plate at the density of 2000/well and treated by different conditions. At the indicated time points, the Premixed WST-1 Reagent (Clontech, Mountain View, CA) was added and incubated at 37°C for 120 min, followed by measuring absorbance at 450 nm.

Flow cytometry analysis of cell apoptosis

1×10^6 cells were treated with different conditions for 48 h and collected in 500 µl PBS.

The collected cells were subjected to Annexin V-FITC and propidium iodide (PI) staining, or Annexin APC-A and DAPI staining. Followed by the cell flow screening and the apoptosis rates were calculated.

Biochemical index test of cells and tissues

The biochemical index were tested by using the Glucose Assay Kit (No. F006-1-1, Nanjing Jiancheng Bioengineering Institute), the Lactic Acid assay kit (No. A019-2-1, Nanjing Jiancheng Bioengineering Institute), the ATP assay kit (No. A095-1-1, Nanjing Jiancheng Bioengineering Institute), the Hexokinase (HK) Assay Kit (No. BC0745, Solarbio), the Pyruvatekinase (PK) Assay Kit (No. BC0545, Solarbio) and the Phosphofructokinase (PFK) Assay Kit (No. BC0535, Solarbio).

Total RNA isolation and touchdown-quantitative real-time PCR (TqPCR) analysis

Total RNA was isolated by using the TRIZOL Reagent (Invitrogen, China) and subjected to reverse transcription into the cDNA products by using hexamer and M-MuLV reverse transcriptase (New England Biolabs, Ipswich, MA). TqPCR was carried out by using 2x SYBR Green qPCR Master Mix (Bimake, Shanghai, China) on the CFX-Connect unit (Bio-Rad Laboratories, Hercules, CA) as described [42]. TqPCR primers were shown in Table S3.

Western blotting analysis

Western blotting assay was carried out as previously described [39]. The primary antibodies against β-ACTIN (1:5000-1:20000 dilution; Proteintech; Cat# 60008-1-Ig), BMP4 (1:1000 dilution; Proteintech; Cat# 12492-1-AP), HK2 (1:2000 dilution; Proteintech; Cat# 22029-1-AP), PFKFB3 (1:1000 dilution; Bimake; Cat# A5593), PKM2 (1:1000 dilution; Bimake; Cat# A5356), SMAD5 (1:1000 dilution; Bimake; Cat# A5511), and p-SMAD5 (phospho S463 + S465; 1:1000 dilution; Abcam; Cat# ab92698), the secondary antibodies (1:5000 dilution; ZSGB-BIG; Peroxidase-Conjugated Rabbit anti-Goat IgG or Peroxidase-Conjugated Goat anti-Mouse IgG, Cat# ZB-2306 or 2305). Immune-reactive signals were visualized with the Enhanced Chemiluminescence (ECL) kit (Millipore, USA) and recorded by using the Bio-Rad ChemiDoc Imager (Hercules, CA). The blots were cropped

and all original, full-length blot images were shown in Figure S3.

Chromatin immunoprecipitation (ChIP) assay

Consensus Smad1/Smad5 binding sites were previously characterized [43, 44]. Numerous putative binding sites for Smad1/Smad5 were found in the promoter regions (e.g., within 2,000 bp upstream of exon 1) of human *HK2*, *PFKM* and *PKM* genes. ChIP assay was conducted to verify these potential binding sites as previously described [45]. Briefly, Hu7 cells were infected with Ad-B4 for 30 h, then cross-linked and subjected to ChIP analysis. Antibody for SMAD5 (1:20 dilution; Bimake; Cat# A5511) was used to pull down the protein-DNA complex. The goat IgG was used as a negative control. The presence of *HK2*, *PFKM* and *PKM* promoter fragments were detected with semi-quantitative PCR using multiple pairs of PCR primers, as listed in Table S4.

Subcutaneous and intrahepatic hepatoma cell implantation in athymic nude mice

The use and care of experimental animals was approved by the Research Ethics and Regulations Committee of Chongqing Medical University. All experimental procedures followed the approved guidelines. The cell implantation experiments were carried out as previously described [39, 46]. Briefly, cells were treated with Ad-B4, Ad-siB4, Ad-GFP or Ad-RFP for 36 h, followed been injected into the flanks of athymic nude mice (5-week old, male, 5×10^6 cells/injection, 4 injections/mouse, 5 mice/group). At 14 days after injection, mice were sacrificed, the intrahepatic tumor masses were retrieved for biochemical indexes detection and IHC staining. Lung metastases nodules were retrieved for IHC staining.

Statistical analysis

All experiments were performed at least three times and/or repeated three batches of independent experiments. Data were analyzed using GraphPad Prism 7 and presented as the mean ± standard deviations (SD). Statistical significance was determined by one-way analysis of variance and the student's t test for the comparisons between groups. A value of *P* < 0.05 was considered statistically significant.

Results

BMP4 is highly expressed in HCC and hepatoma cells tolerant to hypoxia and hypoglycemia

We first determined the expression of BMP4 in human HCC. By taking advantage of the GEO database (http://www.ncbi.nlm.nih.gov/geo/query/acc.cgi?acc=GSE14520), we found that the expression of BMP4 was markedly higher in HCC tumor tissues (T), compared with that in the adjacent liver non-tumor tissue (ALNT) (**Figure 1A**). We further evaluated the protein level of BMP4 in the HCC tumor (T) and ALNT regions in 40 HCC samples by IHC analysis, and found that the immunostaining for BMP4 was stronger and wider in the tumor regions than that in the ALNT regions (**Figure 1B**). As highly metastatic human HCC cell lines, Hu7 and MHCC97H cells have been shown to actively proliferate under the microenvironment of hypoxia and hypoglycemia [47, 48]. We found that the expression of BMP4 was higher in Hu7 and MHCC97H cells than that in human primary hepatocyte (HPH) cells by Western blotting analysis (**Figure 1C**).

We also determined the optimal concentration of $CoCl_2$ for the chemical induction of hypoxia. As shown in Figure S1A, low glucose DMEM and 100 μM $CoCl_2$ were optimal for simulating the hypoxia and hypoglycemia environment in cell culture. Using this culture condition, we validated the higher survival rate and proliferation rate of Hu7 and MHCC97H cells under hypoxia and hypoglycemia condition, compared with that in HPH cells by crystal violet cell viability assay (**Figure 1D**) and WST-1 cell proliferation assay (**Figure 1E**). Furthermore, much lower cell late apoptosis rates were found in Hu7 and MHCC97H cells, compared with that in HPH cells by flow cytometry analysis (**Figure 1F**). These results are supportive of the cell survival advantage of Hu7 and MHCC97H cells in hypoxia and hypoglycemia environment.

BMP4 protects HCC cells from hypoxia and hypoglycemia by promoting proliferation and inhibiting apoptosis

We engineered the recombinant adenoviruses Ad-B4 and Ad-siB4 to overexpress and silence BMP4 respectively. The level of BMP4 overexpression or silencing efficiency of BMP4 expression was firmly validated in Hu7 and MHCC97H
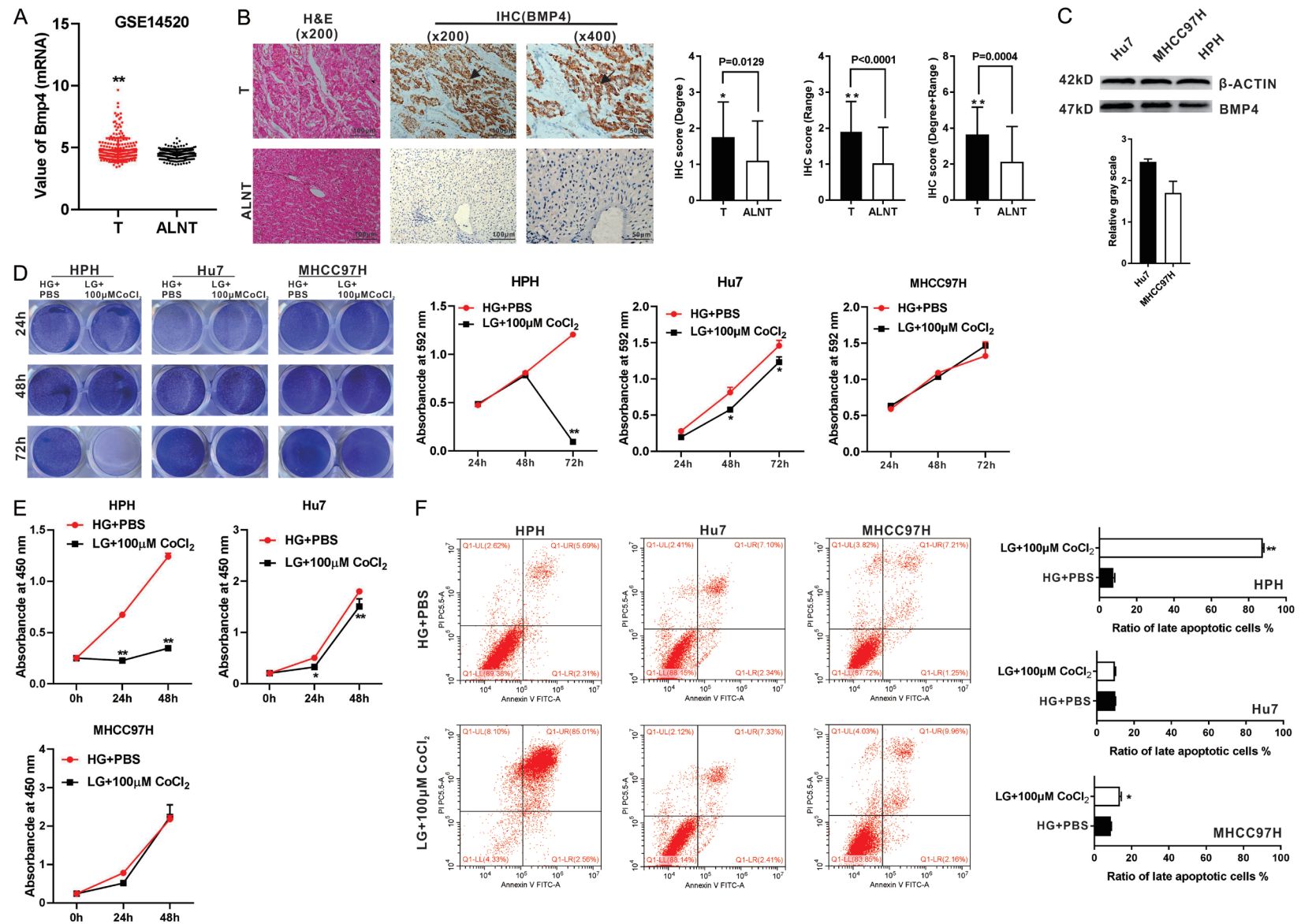
Figure 1. BMP4 is highly expressed in HCC tumor samples and HCC cells. A. BMP4 mRNA expression levels in 225 liver tumor tissues (T) and 220 adjacent liver non-tumor tissue (ALNT) in 225 surgical liver tumor cases (Data from GEO *GSE14520*). B. Paired HCC tumor samples (T) and ALNT samples from 40 patients were evaluated by H & E and IHC (BMP4) under a bright field microscope. Positive stainings were indicated by arrows. The scores of IHC were judged by degree or/and

range of positive staining. "**" P < 0.01, "*" P < 0.05, "T" group vs. "ALNT" group. C. Levels of BMP4 protein expression in the Hu7, MHCC97H and HPH cells were assessed by Western blotting. The cropped blots were shown and Image Lab was used to quantitatively determine the densitometry of original blots. Relative gray scale was calculated by dividing the relative gray values (i.e., BMP4/β-ACTIN). D. Crystal violet staining. HPH, Hu7 and MHCC97H cells were cultured with low glucose (LG) DMED + 100 μM CoCl$_2$, while the culture condition of high glucose (HG) DMED + equal volume PBS was set as a control. Crystal violet cell viability assay and quantitative analysis of crystal violet staining were conducted at 24 h, 48 h and 72 h. "**" P < 0.01, "*" P < 0.05, LG + 100 μM CoCl$_2$ cultured group vs. HG + PBS cultured group. E. WST-1 assay. HPH, Hu7 and MHCC97H cells were cultured with LG DMED + 100 μM CoCl$_2$, while the culture condition of HG DMED + equal volume PBS was set as a control. WST-1 was performed at 0 h, 24 h and 48 h. "**" P < 0.01, "*" P < 0.05, LG + 100 μM CoCl$_2$ cultured group vs. HG + PBS cultured group. F. Flow cytometry analysis. HPH, Hu7 and MHCC97H cells were cultured with LG DMED + 100 μM CoCl$_2$, while the culture condition of HG DMED + equal volume PBS was set as a control. Flow cytometry of cell apoptosis was tested and the ratio of late apoptotic cells (%) was calculated at 48 h. "**" P < 0.01, "*" P < 0.05, LG + 100 μM CoCl$_2$ cultured group vs. HG + PBS cultured group.

cells (Figure S1B and S1C). When Hu7 and MHCC97H cells were cultured under hypoxia and hypoglycemia, and treated with Ad-B4 and Ad-siB4, respectively, crystal violet cell viability assay (**Figure 2A**) and WST-1 cell proliferation assay (**Figure 2B**) indicated that BMP4 promoted cell proliferation for both Hu7 and MHCC97H cells. Flow cytometry analysis revealed that BMP4 reduced cell late apoptosis rate of Hu7 and MHCC97H cells (**Figure 2C**). Thus, these results indicated that BMP4 could protect Hu7 and MHCC97H cells under hypoxia and hypoglycemia conditions.

BMP4 promotes glycolysis of HCC cells under hypoxia and hypoglycemia

We next investigated the effect of BMP4 on glycolysis in HCC cells under hypoxia and hypoglycemia. Hu7 and MHCC97H cells were infected with Ad-B4 and Ad-siB4 respectively, under hypoxia and hypoglycemia. We found BMP4 promoted the glucose uptake (**Figure 3A**), LA (lactic acid) production (**Figure 3B**) and ATP level (**Figure 3C**) in the Hu7 and MHCC97H cells under hypoxia and hypoglycemia. We further tested the activities of rate limiting enzymes of glycolysis, and found that BMP4 also increased the activities of HK (**Figure 3D**), PFK (**Figure 3E**) and PK (**Figure 3F**). In sum, these results strongly suggest that BMP4 may promote glycolysis in Hu7 and MHCC97H cells to accommodate the demand of cellular energy consumption under hypoxia and hypoglycemia.

BMP4 up-regulates the expression of HK2, PFKFB3 and PKM2 through activating Smad signal pathway in HCC cells under hypoxia and hypoglycemia

To understand the possible mechanism underlying BMP4-regulated glycolysis, we first confirmed that the expression of HK2, PFKFB3 and PKM2 were much higher in the HCC tumor regions than that in the ALNT regions (Figure S1D). Then we found that BMP4 up-regulated the expression of HK2, PFK and PKM both at 36 h and 72 h in Hu7 and MHCC97H cells under hypoxia and hypoglycemia by using qPCR analysis (**Figure 4A**). Western blotting also shown that BMP4 up-regulated the protein levels of HK2, PFK and PKM in Hu7 and MHCC97H cells (**Figure 4B**).

Conversely, we found that the BMP type I receptor inhibitor LDN193189 effectively blocked the BMP4-induced increase of glucose uptake (**Figure 5A**), LA (lactic acid) production (**Figure 5B**), ATP level (**Figure 5C**), activity of HK (**Figure 5D**), activity of PFK (**Figure 5E**) and activity of PK (**Figure 5F**) in Hu7 and MHCC97H cells under hypoxia and hypoglycemia. We found BMP4 up-regulated the expression of Smad1/5/8 and Smad6/7 in Hu7 and MHCC97H cells under hypoxia and hypoglycemia (**Figure 5G**). These results demonstrated that BMP4 induced the expression of HK2, PFKFB3 and PKM2 through activating Smad signal pathway in HCC cells under hypoxia and hypoglycemia.

SMAD5 directly binds to the promoter of PKM in HCC cells under hypoxia and hypoglycemia

As SMAD1/5/8 function as important downstream transcription factors of BMP4 and regulate the expression of downstream genes, we demonstrated that BMP4 up-regulated the protein level and phosphorylation level of SMAD5 in the Hu7 and MHCC97H cells under hypoxia and hypoglycemia (**Figure 5H**). We performed ChIP analysis to determine whether Smad1/5 directly bound to the promoters of the rate-limiting glycolysis enzymes. Based on the reported
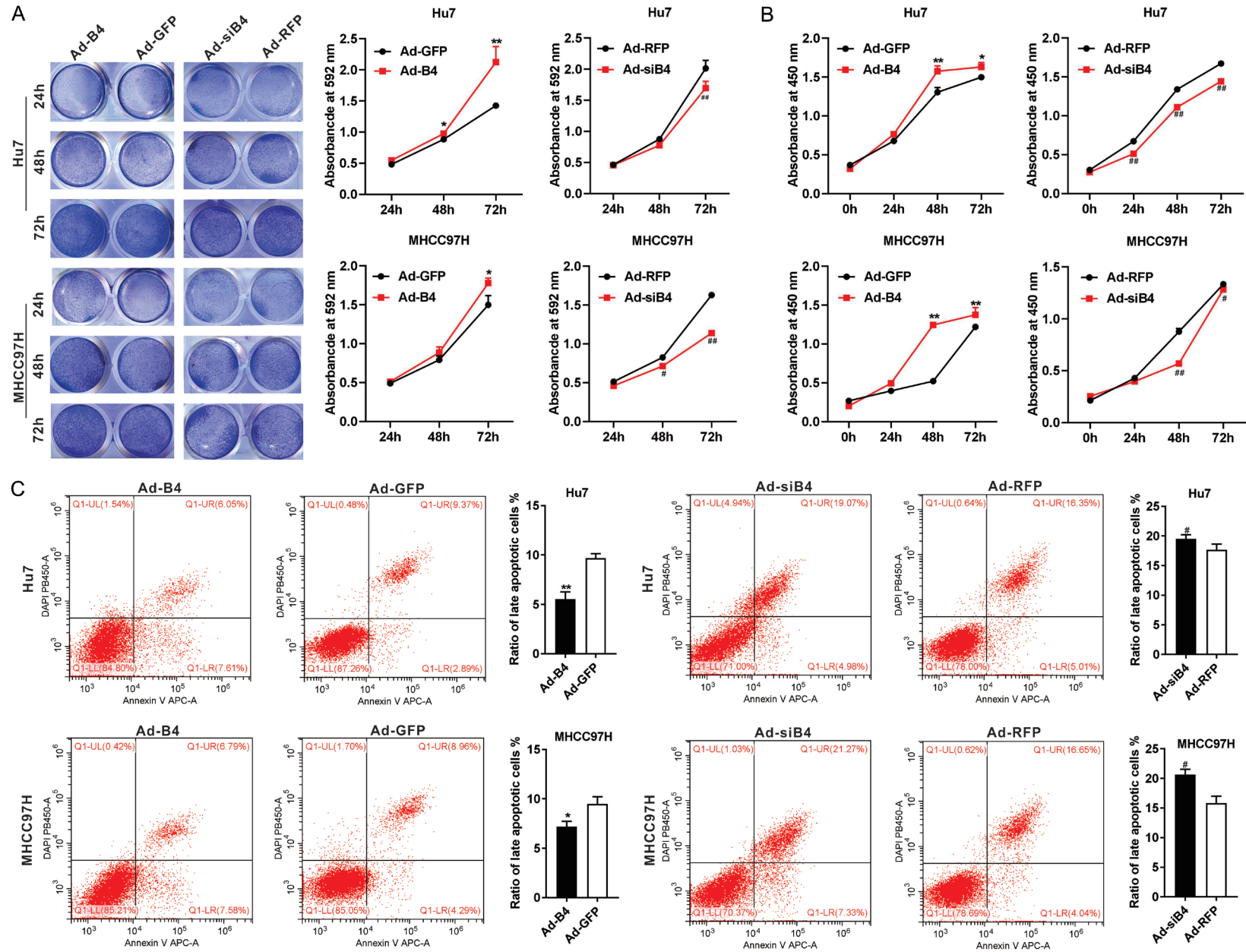
Figure 2. BMP4 promotes proliferation and inhibits apoptosis of HCC cells under hypoxia and hypoglycemia. A. Hu7 and MHCC97H cells were infected with Ad-B4, Ad-GFP, Ad-siB4 and Ad-RFP respectively, and cultured with low glucose (LG) DMED + 100 μM $CoCl_2$, crystal violet cell viability assay and quantitative analysis of crystal violet staining were carried out at 24 h, 48 h and 72 h. "**" $P < 0.01$, "*" $P < 0.05$, Ad-B4 group vs. Ad-GFP group, "##" $P < 0.01$, "#" $P < 0.05$, Ad-siB4 group vs. Ad-RFP group. B. Hu7 and MHCC97H cells were infected with Ad-B4, Ad-GFP, Ad-siB4 and Ad-RFP respectively, and cultured with low glucose (LG) DMED + 100 μM $CoCl_2$, WST-1 assay was done to at 0 h, 24 h, 48 h, and 72 h. "**" $P < 0.01$, "*" $P < 0.05$, Ad-B4 group vs. Ad-GFP group, "##" $P < 0.01$, "#" $P < 0.05$, Ad-siB4 group vs. Ad-RFP group. C. Hu7 and MHCC97H cells were infected with Ad-B4, Ad-GFP, Ad-siB4 and Ad-RFP respectively, and cultured with low glucose (LG) DMED + 100 μM $CoCl_2$, flow cytometry analysis was conducted, and the ratio of late apoptotic cells (%) was calculated at 48 h. "**" $P < 0.01$, "*" $P < 0.05$, Ad-B4 group vs. Ad-GFP group, "#" $P < 0.05$, Ad-siB4 group vs. Ad-RFP group.

consensus SMAD1/5 binding sites, we identified numerous putative binding sites in the 2kb promoter regions of *HK2, PFKM* and *PKM*. ChIP assay results shown that SMAD5 directly bound to the promoter region of *PKM* in the Hu7 cells under hypoxia and hypoglycemia (**Figure 5I**) although further in-depth analyses of SMAD binding ability to these genes' promoter regions, including ChIP-seq and reporter assays, are warranted.

BMP4 promotes glycolysis of HCC cells in vivo

To further validate the impact of BMP4 on glucose metabolic reprogramming in HCC cells, Hu7 and MHCC97H cells infected with Ad-B4 or Ad-siB4 were injected intrahepatically and subcutaneous into athymic nude mice. And we found that in the freshly retrieved tumor samples BMP4 was shown to promote the glucose uptake (**Figure 6A**), LA (lactic acid) production (**Figure 6B**), ATP level (**Figure 6C**), HK activity (**Figure 6D**), PFK activity (**Figure 6E**) and the PK activity (**Figure 6F**). The retrieved tumor samples were subjected to IHC staining, and the expression of HK2, PFKFB3, PKM2, SMAD5 and p-SMAD5 were significantly up-regulated by BMP4, compared with that in the Ad-GFP control groups or the Ad-siB4 groups (**Figure 6G**). Furthermore, we found that the expression of PFKFB3, PKM2 in mouse lung Hu7 cells' metastases, and the expression of HK2, PKM2 in mouse lung MHCC97H cells' metastases were both increased by BMP4 (Figure S2).

Discussion

The mainly metabolic alternations in HCC include gluconeogenesis, elevated glycolysis, β-oxidation, and reduced of tricarboxylic acid cycle and Δ-12 desaturase by using a non-targeted metabolic profiling strategy [49]. Under aerobic condition, most normal cells metabolize glucose to carbon dioxide mainly through

glycolysis and pyruvate oxidation in the mitochondrial tricarboxylic acid (TCA) cycle. This reaction produces NADH, which promotes oxidative phosphorylation to maximize ATP production and minimize lactic acid production. In contrast, most cancer cells produce large amounts of lactate regardless of the availability of oxygen, referred to as "aerobic glycolysis". Thanks to the aerobic glycolysis of tumor cells, most tumor cells are relatively more tolerant to hypoxia and low glucose microenvironment [2, 50]. In this study, we confirmed that the two aggressive HCC lines Hu7 and MHCC97H were tolerant to hypoxia and hypoglycemia.

Recent studies shown that BMP4 was highly expressed in liver among BMPs and play multiple effects on HCC. BMP4 enhanced HCC proliferation by promoting cell cycle via ID2/CDKN1B signaling, promoted metastasis of HCC by inducing EMT through up regulating ID2, provided cancer-supportive phenotypes to liver fibroblasts in patients with HCC, and increase proliferation and migration of HCC by active MEK/ERK signaling pathway [46, 51-53]. However, BMP4 also induced differentiation of CD133+ hepatic cancer stem cells, blocked their contributions to HCC [54]. Here, we found BMP4 is highly expressed in HCC samples and the Hu7 and MHCC97H cells, and protects HCC cells from hypoxia and hypoglycemia by promotes proliferation and inhibits apoptosis. On the other hand, BMP4 plays an important role in the regulation of glucose metabolism. BMP4-BMPR1A signaling pathway in β cells is a necessary condition for regulating insulin secretion [20].

BMP4 can mediated brown fat-like changes into white adipose tissue to change the homeostasis of glucose and energy [55]. Nonetheless, the potential impact of BMP4 on glucose metabolic reprogramming HCC cells remains to be fully understood.
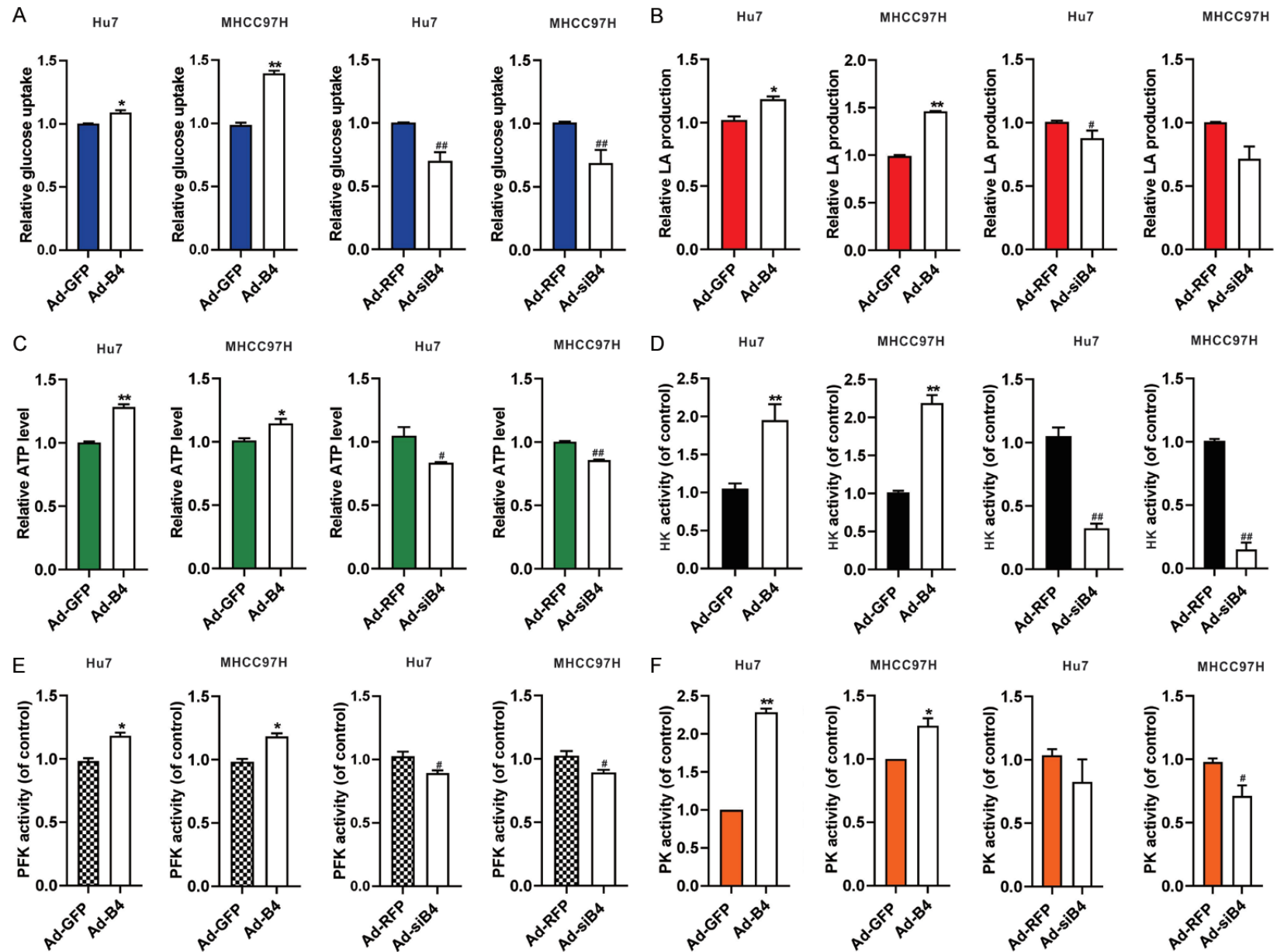
Figure 3. BMP4 promotes glycolysis of HCC cells under hypoxia and hypoglycemia. Hu7 and MHCC97H cells were infected with Ad-B4, Ad-GFP, Ad-siB4 and Ad-RFP, respectively, and cultured with low glucose (LG) DMED + 100 μM CoCl$_2$. The glucose uptake (A), LA (lactic acid) production (B), ATP level (C), activity of HK (D), activity of PFK (E) and activity of PK (F) were assessed at 48 h. "**" P < 0.01, "*" P < 0.05, Ad-B4 group vs. Ad-GFP group, "##" P < 0.01, "#" P < 0.05, Ad-siB4 group vs. Ad-RFP group.
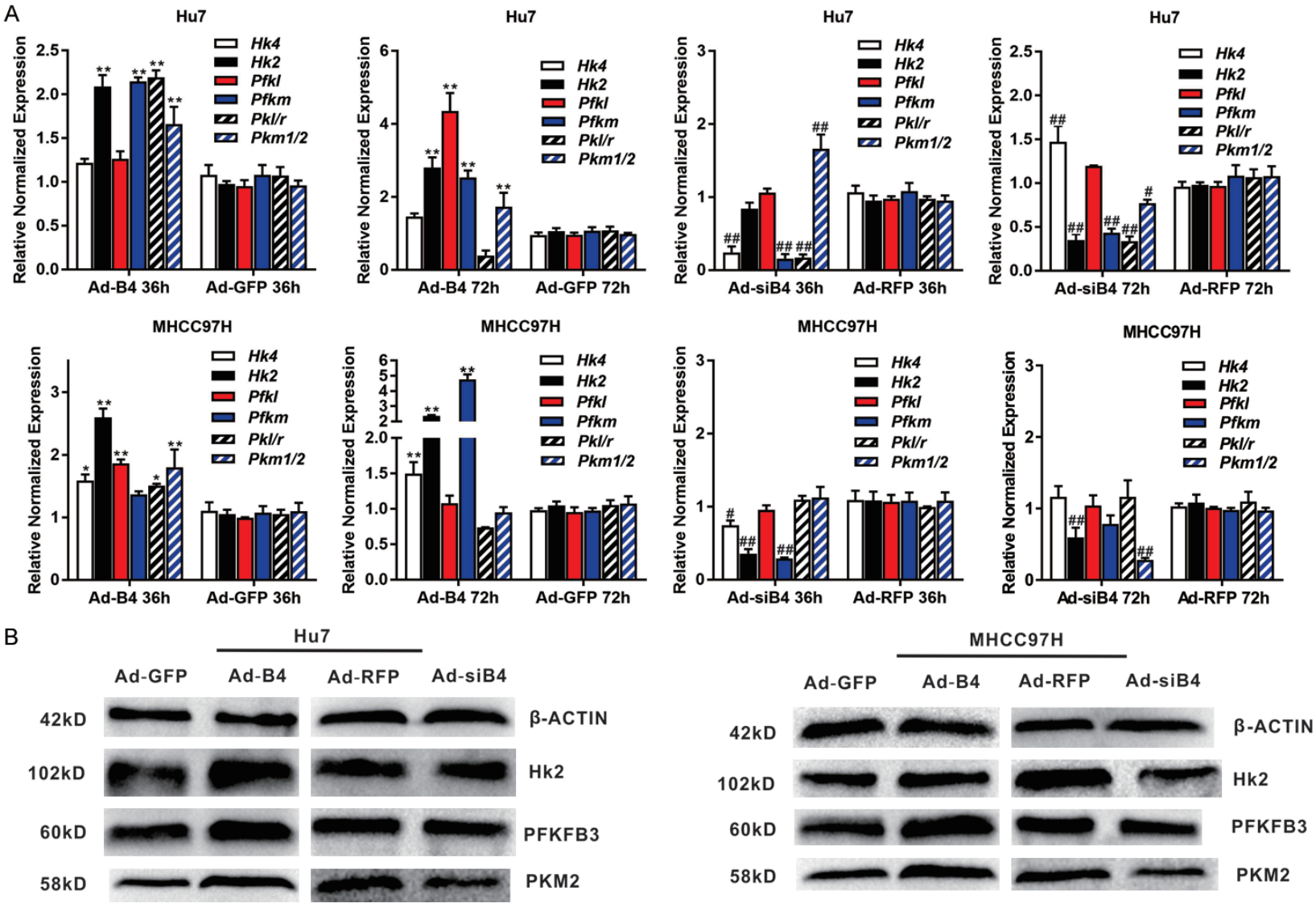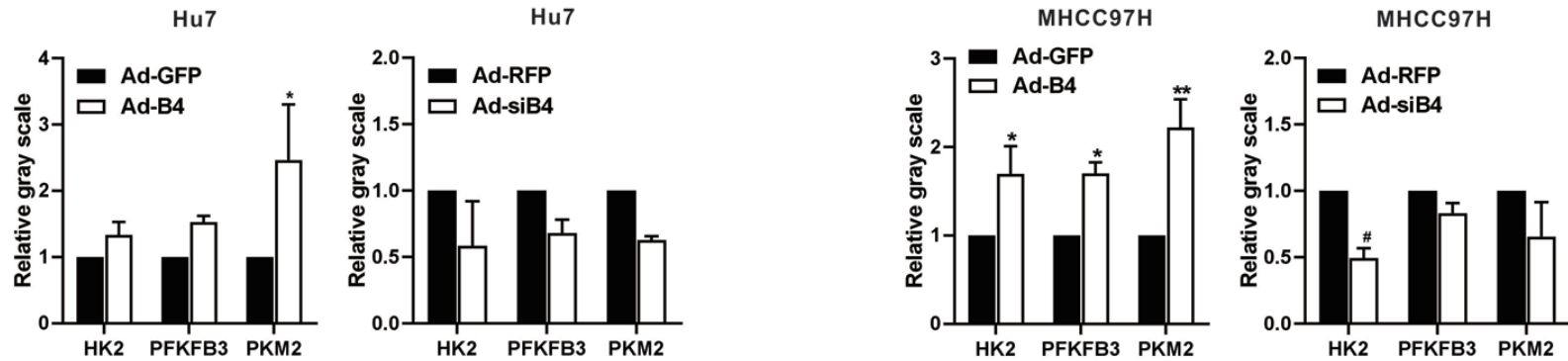
Figure 4. BMP4 up-regulates the expression of glycolysis rate limiting enzymes in HCC cells under hypoxia and hypoglycemia. Hu7 and MHCC97H cells were infected with Ad-B4, Ad-GFP, Ad-siB4 and Ad-RFP, respectively, and cultured with low glucose (LG) DMED + 100 μM CoCl$_2$. A. TqPCR analysis was carried out to detect the expression of glycolysis rate limiting enzymes at 36 h and 72 h. "**" P < 0.01, "*" P < 0.05, Ad-B4 group vs. Ad-GFP group, "##" P < 0.01, "#" P < 0.05, Ad-siB4 group vs. Ad-RFP group. B. Western blotting was used to assess the expression of HK2, PFKFB3 and PKM2 at 72 h. The cropped blots were shown and Image Lab was used to quantitatively determine the densitometry of original blots. Relative gray scale was calculated by dividing the relative gray values (i.e., HK2/ β-ACTIN) in "**" P < 0.01, "*" P < 0.05, Ad-B4 group vs. Ad-GFP group, "#" P < 0.05, Ad-siB4 group vs. Ad-RFP group.
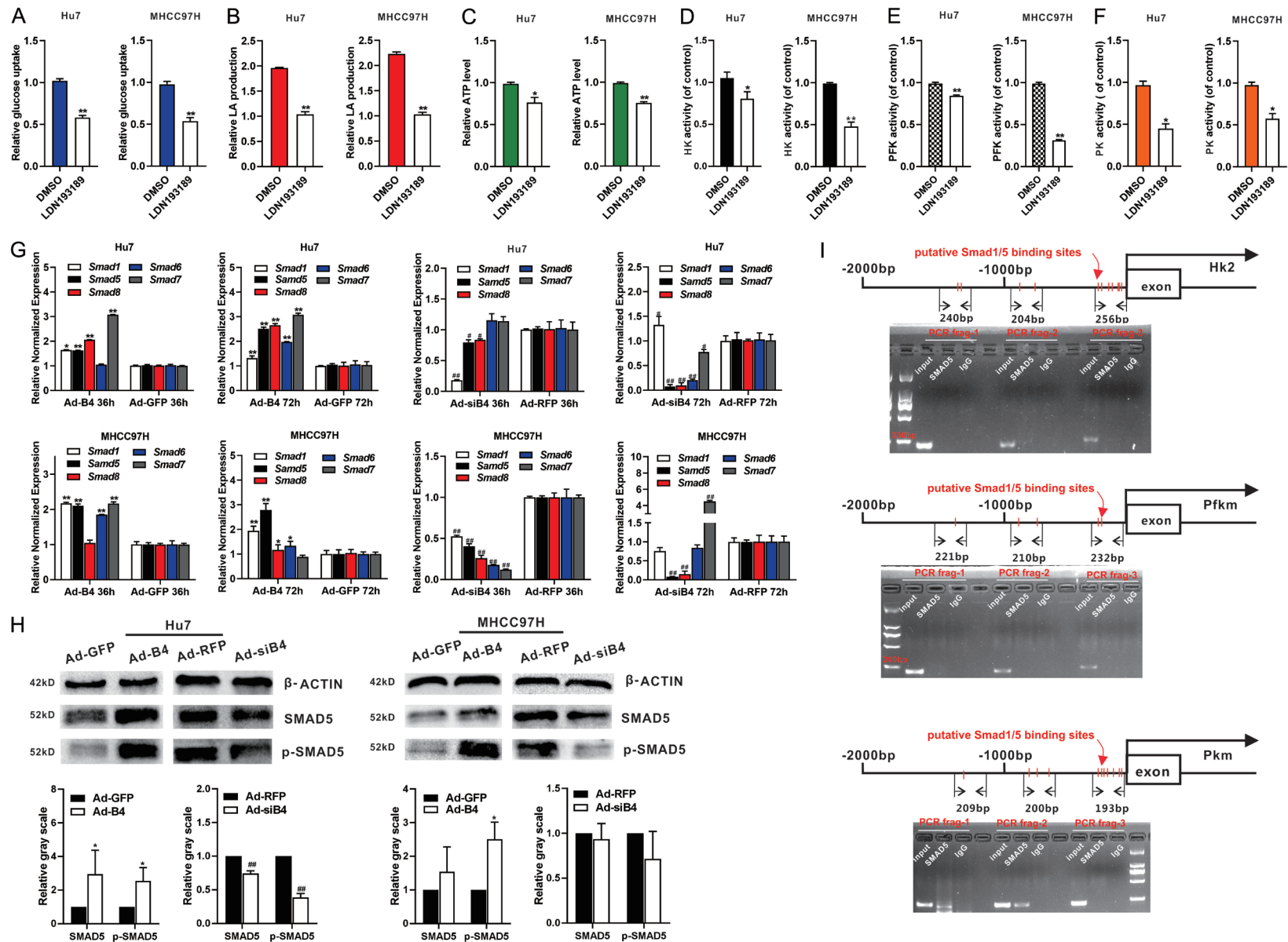
Figure 5. BMP4 up-regulates the expression of HK2, PFKFB3 and PKM2 through activating canonical BMP/SMAD signal pathway, and SMAD5 can directly bind to the promoter of PKM under hypoxia and hypoglycemia. Hu7 and MHCC97H cells were infected with Ad-B4 and LDN193189 under hypoxia and hypoglycemia. The

glucose uptake (A), LA (lactic acid) production (B), ATP level (C), activity of HK (D), activity of PFK (E) and activity of PK (F) were measured at 48 h. "**" P < 0.01, "*" P < 0.05, LDN193189 group vs. DMSO group. (G) Hu7 and MHCC97H cells were infected with Ad-B4 and Ad-siB4 under hypoxia and hypoglycemia, TqPCR analysis was carried out to detect the expression of SMAD1, 5, 6, 7, 8 at 36 h and 72 h. "**" P < 0.01, "*" P < 0.05, Ad-B4 group vs. Ad-GFP group, "##" P < 0.01, "#" P < 0.05, Ad-siB4 group vs. Ad-RFP group. (H) Western blotting was used to detect the protein and phosphorylation level of SMAD5. The cropped blots were shown and Image Lab was used to quantitatively determine the densitometry of original blots. Relative gray scale was calculated by dividing the relative gray values (i.e., SMAD5/β-ACTIN) in "*" P < 0.05, Ad-B4 group vs. Ad-GFP group. "##" P < 0.01, Ad-siB4 group vs. Ad-RFP group. (I) For ChIP assay of Smad5, three pairs of PCR primers were designed to check the possible binding sites in the promoters of HK2, PFKM and PKM after Ad-B4 infection for 30 h in Hu7 cells with low glucose (LG) DMED + 100 μM CoCl$_2$.
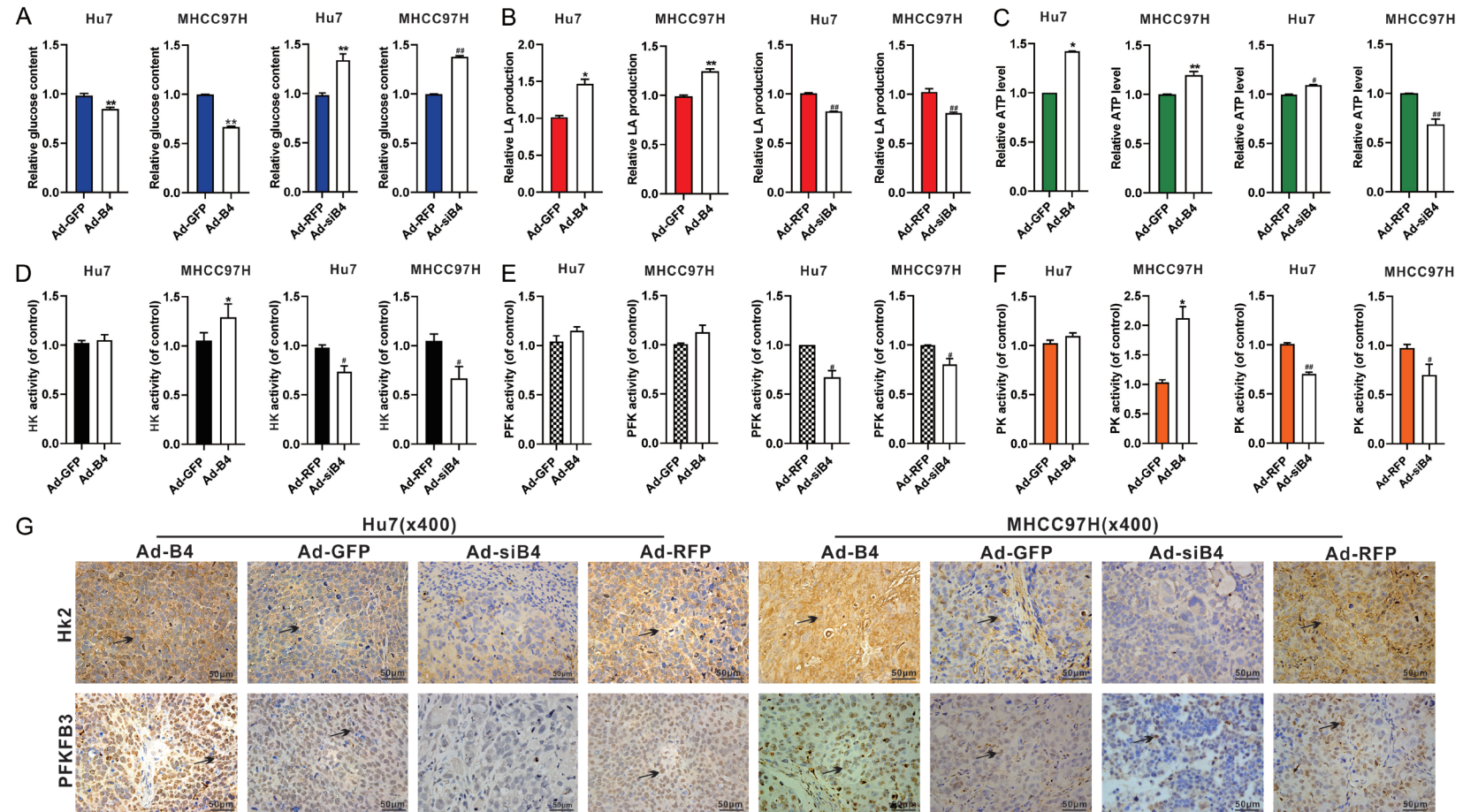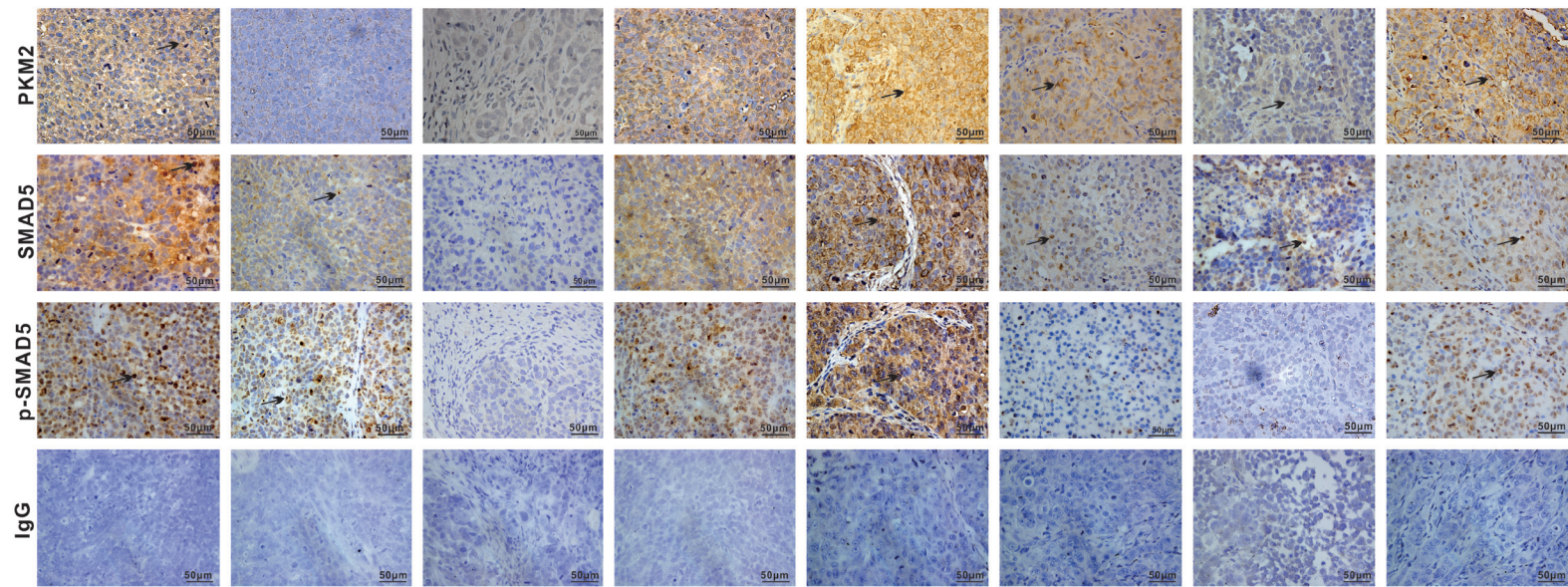
Figure 6. BMP4 promotes glycolysis of HCC cells *in vivo*. Hu7 and MHCC97H cells were infected with Ad-B4 and Ad-siB4, then injected intra-hepatically subcutaneously and into nude mice. The mice were sacrificed after 14 days. The retrieved tumor samples were subjected to assess the glucose content (A), LA (lactic acid) production (B), ATP level (C), activity of HK (D), activity of PFK (E) and activity of PK (F). "**" P < 0.01, "*" P < 0.05, Ad-B4 group vs. Ad-GFP group, "##" P < 0.01, "#" P < 0.05, Ad-siB4 group vs. Ad-RFP group. (G) The retrieved tumor samples were subjected to IHC staining to assess the expression of HK2, PFKFB3, PKM2, SMAD5 and p-SMAD5. Results were observed under a bright field microscope (×400), and positive staining were indicated by arrows. Representative results were shown.

It is rather challenging to understand the precise mechanisms through which tumors adapt to hypoxia and hypoglycemia microenvironment. The structure and function of tumor vascular system are abnormal. In addition, the internal changes of tumor cell metabolism cause the creates spatial and temporal heterogeneity of oxygenation, pH value, glucose and many other metabolites [56]. In the process of tumorigenesis, the loss of tumor suppressor may lead to cell over metabolism and redox imbalance. It has been reported that NADPH is produced during the conversion of isocitric acid to α- ketoglutarate (αKG) catalyzed by isocitrate dehydrogenase 1 (IDH1) and IDH2, and mutations in IDH1 and IDH2 are associated with tumorigenesis [57]. P53 can promote oxidative stress and induce apoptosis. Retinoblastoma (rb) normally participates in the antioxidant response. Myc not only promotes proliferation, but also promotes the production of accompanying macromolecules and antioxidants needed for growth and during the process of tumorigenesis. Loss of PTEN and overexpression of AKT1 resulted in FOXO inactivation and increased oxidative stress [58]. HIF1 amplification encodes gene transcription of glucose transporters and most glycolytic enzymes, increasing the ability of cells to carry out glycolysis. Loss of tumor suppressors may cause cells to become overloaded with the products of aberrant metabolism and redox imbalance [59-61]. In addition, mutations in oncogenes and tumor suppressor genes result in changes in many intracellular signaling pathways including PI3K pathway [62].

In our study, we found BMP4 promoted glycolysis of HCC cells under hypoxia and hypoglycemia, including increased the glucose uptake, lactic acid production and ATP level. The rate limiting enzymes of glycolysis play important role in liver cancer. HK2 mRNA expression was significantly higher in metastatic liver cancers [63]. HK2 is essential for glycolysis of HCC and HK2 depletion induces oxidative phosphorylation in [64]. Inhibited the expression of HK2 can reduce aerobic glycolysis and tumor growth in HCC [65]. Overexpression of PKM2 in tumor tissues is associated with poor prognosis in patients with HCC [66]. Inhibited the activity of PFK induced the apoptosis of HCC [67]. We further found BMP4 also increased the activities and expression of HK, PFK and PKM in Hu7 and HMCC97H cells under hypoxia and hypoglycemia.

BMP4 functions through binding to the receptors BMPR-II, ALK-3 and/or ALK-6, and activates Smad1, 5, 8 that interact with Smad4. The Smad complex is translocated into the nucleus, and interact with transcription factors to regulate the expression of downstream genes [68, 69]. We found that BMP type I receptor inhibitor LDN193189 effectively blocked the effect of BMP4 on glycolysis and up-regulated expression of Smad1/5/8. ChIP assay results showed that SMAD5 directly bound to the promoter region of PKM in HCC cells.

In sum, we demonstrated that BMP4 protected HCC cells from hypoxia and hypoglycemia by promoting glycolysis through a direct regulation of the rate limiting enzymes of glycolysis via the canonical Smad signal pathway. Our findings suggest that BMP4 may play an important role in regulating glycolysis of HCC cells under hypoxia and hypoglycemia condition, indicating that novel therapeutics may be developed to target BMP4-regulated glucose metabolic reprogramming in HCC.

Disclosure of conflict of interest

None.

Authors' contribution

Jiaming Fan and Tongchuan He: Conceived the project and oversaw the study, reviewed and approved the manuscript, provided the research funds; Jiamin Zhong: Performed most of the experiments in vitro and in vivo, collected and analysis data, original draft, wrote the

manuscript; Piao Zhao and Yannian Gou: Performed part of the experiments in vitro; Yetao Luo: Data analysis and statistical analysis; Quan Kang, Youde Cao, and Baicheng He: Provided essential experimental supports and important research resources.

Abbreviations

HCC, Hepatocellular carcinoma; BMPs, Bone morphogenetic proteins; DMEM, Dulbecco's modified eagle medium; FBS, fetal bovine serum; HPH, Human primary hepatocytes; T, tumor tissue; ALNT, Adjacent liver non-tumor tissue; Ad-B4, Adenoviral vector expressing human BMP4; Ad-GFP, Adenoviral vector expressing the green fluorescent protein (GFP); Ad-siB4, Adenoviral vector expressing three siRNAs that silence human Bmp4; Ad-RFP, Adenoviral vector expressing the red fluorescent protein (RFP); H & E, hematoxylin and eosin; IHC, immunohistochemistry; TqPCR, touchdown quantitative real-time PCR; HK2, hexokinase 2; PKM, pyruvate kinase M1/2; PFK, Phosphofructokinase.

Address correspondence to: Dr. Jiaming Fan, Ministry of Education Key Laboratory of Diagnostic Medicine, Department of Clinical Biochemistry, School of Laboratory Medicine, Chongqing Medical University, No. 1 Medical School Road, Yuzhong District, Chongqing 400016, China. Tel: +86-023-68485240; E-mail: fanjiaming1988@cqmu.edu.cn

References

[1] Ai-Wu S, Yuan-Sheng C and Li LIJG. Hepatocellular carcinoma. Gastroenterologist 2016; 20: 703-720.

[2] Heiden MGV, Cantley LC and Thompson CB. Understanding the warburg effect: the metabolic requirements of cell proliferation. Science 2009; 324: 1029-1033.

[3] Bechmann LP, Hannivoort RA, Gerken G, Hotamisligil GS, Trauner M and Canbay A. The interaction of hepatic lipid and glucose metabolism in liver diseases. J Hepatol 2012; 56: 952-964.

[4] Cairns RA, Harris IS and Mak TW. Regulation of cancer cell metabolism. Nature Reviews Cancer 2011; 11: 85-95.

[5] Pavlova NN and Thompson CB. The emerging hallmarks of cancer metabolism. Cell Metab 2016; 23: 27-47.

[6] Vander Heiden MG and DeBerardinis RJ. Understanding the intersections between metabolism and cancer biology. Cell 2017; 168: 657-669.

[7] Semenza GL. Targeting HIF-1 for cancer therapy. Nat Rev Cancer 2003; 3: 721-732.

[8] Derynck R and Zhang YE. Smad-dependent and Smad-independent pathways in TGF-beta family signalling. Nature 2003; 425: 577-584.

[9] Luu HH, Song WX, Luo X, Manning D, Luo J, Deng ZL, Sharff KA, Montag AG, Haydon RC and He TC. Distinct roles of bone morphogenetic proteins in osteogenic differentiation of mesenchymal stem cells. J Orthop Res 2007; 25: 665-677.

[10] Wang RN, Green J, Wang Z, Deng Y, Qiao M, Peabody M, Zhang Q, Ye J, Yan Z, Denduluri S, Idowu O, Li M, Shen C, Hu A, Haydon RC, Kang R, Mok J, Lee MJ, Luu HL and Shi LL. Bone morphogenetic protein (BMP) signaling in development and human diseases. Genes Dis 2014; 1: 87-105.

[11] Weiss A and Attisano L. The TGFbeta superfamily signaling pathway. Wiley Interdiscip Rev Dev Biol 2013; 2: 47-63.

[12] Salazar VS, Gamer LW and Rosen V. BMP signalling in skeletal development, disease and repair. Nat Rev Endocrinol 2016; 12: 203-221.

[13] Shimasaki S, Moore RK, Otsuka F and Erickson GF. The bone morphogenetic protein system in mammalian reproduction. Endocr Rev 2004; 25: 72-101.

[14] Ma J, Zeng S, Zhang Y, Deng G, Qu Y, Guo C, Yin L, Han Y and Shen H. BMP4 enhances hepatocellular carcinoma proliferation by promoting cell cycle progression via ID2/CDKN1B signaling. Mol Carcinog 2017; 56: 2279-2289.

[15] Ma J, Zeng S, Zhang Y, Deng G, Qu Y, Guo C, Yin L, Han Y, Cai C, Li Y, Wang G, Bonkovsky HL and Shen H. BMP4 promotes oxaliplatin resistance by an induction of epithelial-mesenchymal transition via MEK1/ERK/ELK1 signaling in hepatocellular carcinoma. Cancer Lett 2017; 411: 117-129.

[16] Li X, Gao L, Zheng L, Shi J and Ma J. BMP4-mediated autophagy is involved in the metastasis of hepatocellular carcinoma via JNK/Beclin1 signaling. Am J Transl Res 2020; 12: 3068-3077.

[17] Li X, Sun B, Zhao X, An J, Zhang Y, Gu Q, Zhao N, Wang Y and Liu F. Function of BMP4 in the formation of vasculogenic mimicry in hepatocellular carcinoma. J Cancer 2020; 11: 2560-2571.

[18] Mostafa S, Pakvasa M, Coalson E, Zhu A, Alverdy A, Castillo H, Fan J, Li A, Feng Y, Wu D, Bishop E, Du S, Spezia M, Li A, Hagag O, Deng A, Liu W, Li M, Ho SS, Athiviraham A, Lee MJ, Wolf JM, Ameer GA, Luu HH, Haydon RC, Strelzow J, Hynes K, He TC and Reid RR. The wonders of BMP9: from mesenchymal stem cell differentiation, angiogenesis, neurogenesis, tumorigenesis, and metabolism to regenerative medicine. Genes Dis 2019; 6: 201-223.

[19] Miyazawa K and Miyazono K. Regulation of TGF-β family signaling by inhibitory smads. Cold Spring Harb Perspect Biol 2017; 9: a022095.

[20] Goulley J, Dahl U, Baeza N, Mishina Y and Edlund H. BMP4-BMPR1A signaling in beta cells is required for and augments glucose-stimulated insulin secretion. Cell Metabolism 2007; 5: 207-219.

[21] Zhang Y, Liu J, Tian XY, Wong WT and Huang Y. Inhibition of bone morphogenic protein 4 restores endothelial function in db/db diabetic mice. Arterioscler Thromb Vasc Biol 2014; 34: 152-159.

[22] Wei Q, Fan J, Liao J, Zou Y, Song D, Liu J, Cui J, Liu F, Ma C, Hu X, Li L, Yu Y, Qu X, Chen L, Yu X, Zhang Z, Zhao C, Zeng Z, Zhang R, Yan S, Wu X, Shu Y, Reid RR, Lee MJ, Wolf JM and He TC. Engineering the rapid adenovirus production and amplification (RAPA) cell line to expedite the generation of recombinant adenoviruses. Cell Physiol Biochem 2017; 41: 2383-2398.

[23] Wu N, Zhang H, Deng F, Li R, Zhang W, Chen X, Wen S, Wang N, Zhang J, Yin L, Liao Z, Zhang Z, Zhang Q, Yan Z, Liu W, Wu D, Ye J, Deng Y, Yang K, Luu HH, Haydon RC and He TC. Overexpression of Ad5 precursor terminal protein accelerates recombinant adenovirus packaging and amplification in HEK-293 packaging cells. Gene Ther 2014; 21: 629-637.

[24] Piret JP, Mottet D, Raes M and Michiels C. CoCl2, a chemical inducer of hypoxia-inducible factor-1, and hypoxia reduce apoptotic cell death in hepatoma cell line HepG2. Ann N Y Acad Sci 2010; 973: 443-447.

[25] Piret JP, Lecocq C, Toffoli S, Ninane N, Raes M and Michiels C. Hypoxia and CoCl2 protect HepG2 cells against serum deprivation- and t-BHP-induced apoptosis: a possible anti-apoptotic role for HIF-1. Exp Cell Res 2004; 295: 340-349.

[26] Fan J, Wei Q, Liao J, Zou Y, Song D, Xiong D, Ma C, Hu X, Qu X, Chen L, Li L, Yu Y, Yu X, Zhang Z, Zhao C, Zeng Z, Zhang R, Yan S, Wu T, Wu X, Shu Y, Lei J, Li Y, Zhang W, Haydon RC, Luu HH, Huang A, He TC and Tang H. Noncanonical Wnt signaling plays an important role in modulating canonical Wnt-regulated stemness, proliferation and terminal differentiation of hepatic progenitors. Oncotarget 2017; 8: 27105-27119.

[27] Huang E, Bi Y, Jiang W, Luo X, Yang K, Gao JL, Gao Y, Luo Q, Shi Q, Kim SH, Liu X, Li M, Hu N, Liu H, Cui J, Zhang W, Li R, Chen X, Shen J, Kong Y, Zhang J, Wang J, Luo J, He BC, Wang H, Reid RR, Luu HH, Haydon RC, Yang L and He TC. Conditionally immortalized mouse embryonic fibroblasts retain proliferative activity without compromising multipotent differentiation potential. PLoS One 2012; 7: e32428.

[28] Cui J, Zhang W, Huang E, Wang J, Liao J, Li R, Yu X, Zhao C, Zeng Z, Shu Y, Zhang R, Yan S, Lei J, Yang C, Wu K, Wu Y, Huang S, Ji X, Li A, Gong C, Yuan C, Zhang L, Liu W, Huang B, Feng Y, An L, Zhang B, Dai Z, Shen Y, Luo W, Wang X, Huang A, Luu HH, Reid RR, Wolf JM, Thinakaran G, Lee MJ and He TC. BMP9-induced osteoblastic differentiation requires functional Notch signaling in mesenchymal stem cells. Lab Invest 2019; 99: 58-71.

[29] Xian J, Cheng Y, Qin X, Cao Y, Luo Y and Cao Y. Progress in the research of p53 tumour suppressor activity controlled by Numb in triple-negative breast cancer. J Cell Mol Med 2020; 24: 7451-7459.

[30] Luo J, Deng ZL, Luo X, Tang N, Song WX, Chen J, Sharff KA, Luu HH, Haydon RC, Kinzler KW, Vogelstein B and He TC. A protocol for rapid generation of recombinant adenoviruses using the AdEasy system. Nat Protoc 2007; 2: 1236-1247.

[31] Peng Q, Chen B, Wang H, Zhu Y and Fan J. Bone morphogenetic protein 4 (BMP4) alleviates hepatic steatosis by increasing hepatic lipid turnover and inhibiting the mTORC1 signaling axis in hepatocytes. Aging 2019; 11: 11520-11540.

[32] Kang Q, Song WX, Luo Q, Tang N, Luo J, Luo X, Chen J, Bi Y, He BC, Park JK, Jiang W, Tang Y, Huang J, Su Y, Zhu GH, He Y, Yin H, Hu Z, Wang Y, Chen L, Zuo GW, Pan X, Shen J, Vokes T, Reid RR, Haydon RC, Luu HH and He TC. A comprehensive analysis of the dual roles of BMPs in regulating adipogenic and osteogenic differentiation of mesenchymal progenitor cells. Stem Cells Dev 2009; 18: 545-559.

[33] Luo Q, Kang Q, Song WX, Luu HH, Luo X, An N, Luo J, Deng ZL, Jiang W, Yin H, Chen J, Sharff KA, Tang N, Bennett E, Haydon RC and He TC. Selection and validation of optimal siRNA target sites for RNAi-mediated gene silencing. Gene 2007; 395: 160-169.

[34] Deng F, Chen X, Liao Z, Yan Z, Wang Z, Deng Y, Zhang Q, Zhang Z, Ye J, Qiao M, Li R, Denduluri S, Wang J, Wei Q, Li M, Geng N, Zhao L, Zhou G, Zhang P, Luu HH, Haydon RC, Reid RR, Yang T and He TC. A simplified and versatile system for the simultaneous expression of multiple siRNAs in mammalian cells using Gibson DNA assembly. PLoS One 2014; 9: e113064.

[35] Shu Y, Wu K, Zeng Z, Huang S, Ji X, Yuan C, Zhang L, Liu W, Huang B, Feng Y, Zhang B, Dai Z, Shen Y, Luo W, Wang X, Liu B, Lei Y, Ye Z, Zhao L, Cao D, Yang L, Chen X, Luu HH, Reid RR, Wolf JM, Lee MJ and He TC. A simplified system to express circularized inhibitors of miRNA for stable and potent suppression of miRNA functions. Mol Ther Nucleic Acids 2018; 13: 556-567.

[36] Fan J, Feng Y, Zhang R, Zhang W, Shu Y, Zeng Z, Huang S, Zhang L, Huang B, Wu D, Zhang B,

Wang X, Lei Y, Ye Z, Zhao L, Cao D, Yang L, Chen X, Liu B, Wagstaff W, He F, Wu X, Zhang J, Moriatis Wolf J, Lee MJ, Haydon RC, Luu HH, Huang A, He TC and Yan S. A simplified system for the effective expression and delivery of functional mature microRNAs in mammalian cells. Cancer Gene Ther 2020; 27: 424-437.

[37] Wang X, Yuan C, Huang B, Fan J, Feng Y, Li AJ, Zhang B, Lei Y, Ye Z, Zhao L, Cao D, Yang L, Wu D, Chen X, Liu B, Wagstaff W, He F, Wu X, Luo H, Zhang J, Zhang M, Haydon RC, Luu HH, Lee MJ, Moriatis Wolf J, Huang A, He TC and Zeng Z. Developing a versatile shotgun cloning strategy for single-vector-based multiplex expression of short interfering RNAs (siRNAs) in mammalian cells. ACS Synth Biol 2019; 8: 2092-2105.

[38] Yu X, Chen L, Wu K, Yan S, Zhang R, Zhao C, Zeng Z, Shu Y, Huang S, Lei J, Ji X, Yuan C, Zhang L, Feng Y, Liu W, Huang B, Zhang B, Luo W, Wang X, Liu B, Haydon RC, Luu HH, He TC and Gan H. Establishment and functional characterization of the reversibly immortalized mouse glomerular podocytes (imPODs). Genes Dis 2018; 5: 137-149.

[39] Wang H, Cao Y, Shu L, Zhu Y, Peng Q, Ran L, Wu J, Luo Y, Zuo G, Luo J, Zhou L, Shi Q, Weng Y, Huang A, He TC and Fan J. Long non-coding RNA (lncRNA) H19 induces hepatic steatosis through activating MLXIPL and mTORC1 networks in hepatocytes. J Cell Mol Med 2020; 24: 1399-1412.

[40] Zhang F, Li Y, Zhang H, Huang E, Gao L, Luo W, Wei Q, Fan J, Song D, Liao J, Zou Y, Liu F, Liu J, Huang J, Guo D, Ma C, Hu X, Li L, Qu X, Chen L, Yu X, Zhang Z, Wu T, Luu HH, Haydon RC, Song J, He TC and Ji P. Anthelmintic mebendazole enhances cisplatin's effect on suppressing cell proliferation and promotes differentiation of head and neck squamous cell carcinoma (HNSCC). Oncotarget 2017; 8: 12968-12982.

[41] Deng Y, Wang Z, Zhang F, Qiao M, Yan Z, Wei Q, Wang J, Liu H, Fan J, Zou Y, Liao J, Hu X, Chen L, Yu X, Haydon RC, Luu HH, Qi H, He TC and Zhang J. A Blockade of IGF signaling sensitizes human ovarian cancer cells to the anthelmintic niclosamide-induced anti-proliferative and anticancer activities. Cell Physiol Biochem 2016; 39: 871-888.

[42] Zhang Q, Wang J, Deng F, Yan Z, Xia Y, Wang Z, Ye J, Deng Y, Zhang Z, Qiao M, Li R, Denduluri SK, Wei Q, Zhao L, Lu S, Wang X, Tang S, Liu H, Luu HH, Haydon RC, He TC and Jiang L. TqPCR: a touchdown qPCR assay with significantly improved detection sensitivity and amplification efficiency of SYBR green qPCR. PLoS One 2015; 10: e0132666.

[43] Martin-Malpartida P, Batet M, Kaczmarska Z, Freier R and Macias MJ. Structural basis for genome wide recognition of 5-bp GC motifs by SMAD transcription factors. Nat Commun 2017; 8: 2070.

[44] Masato M, Daizo K, Shuichi T, Eleftheria V, Yasuharu K, Carl-Henrik H, Hiroyuki A and Kohei M. ChIP-seq reveals cell type-specific binding patterns of BMP-specific Smads and a novel binding motif. Nucleic Acids Research 2011; 8712-8727.

[45] Wang H, Hu Y, He F, Li L, Li PP, Deng Y, Li FS, Wu K and He BC. All-trans retinoic acid and COX-2 cross-talk to regulate BMP9-induced osteogenic differentiation via Wnt/β-catenin in mesenchymal stem cells. Biomed Pharmacother 2019; 118: 109279.

[46] Ma J, Zeng S, Zhang Y, Deng G, Qu Y, Guo C, Yin L, Han Y and Shen H. BMP4 enhances hepatocellular carcinoma proliferation by promoting cell cycle progression via ID2/CDKN1B signaling. Mol Carcinog 2017; 56: 2279-2289.

[47] Yang M, Chen Ci, Chau Ga, Chiou S, Su Ce, Chou Ti, Peng Wi and Wu J. Comprehensive analysis of the independent effect of twist and snail in promoting metastasis of hepatocellular carcinoma. Hepatology 2010; 50: 1464-1474.

[48] Yuan R, Wang K, Hu J, Yan C and Shao J. Ubiquitin-like protein FAT10 promotes the invasion and metastasis of hepatocellular carcinoma by modifying β-catenin degradation. Cancer Res 2014; 74: 5287.

[49] Huang Q, Tan Y, Yin P, Ye G, Gao P, Lu X, Wang H and Xu G. Metabolic characterization of hepatocellular carcinoma using nontargeted tissue metabolomics. Cancer Res 2013; 73: 4992-5002.

[50] Koppenol WH, Bounds PL and Dang CV. Otto Warburg's contributions to current concepts of cancer metabolism. Nat Rev Cancer 2011; 11: 325-337.

[51] Chiu CY, Kuo KK, Kuo TL, Lee KT and Cheng KH. The activation of MEK/ERK signaling pathway by bone morphogenetic protein 4 to increase hepatocellular carcinoma cell proliferation and migration. Mol Cancer Res 2012; 10: 415-427.

[52] Zeng S, Zhang Y, Ma J, Deng G, Qu Y, Guo C, Han Y, Yin L, Cai C and Li Y. BMP4 promotes metastasis of hepatocellular carcinoma by an induction of epithelial-mesenchymal transition via upregulating ID2. Cancer Lett 2017; 390: 67-76.

[53] Mano Y, Yoshio S, Shoji H, Tomonari S, Aoki Y, Aoyanagi N, Okamoto T, Matsuura Y, Osawa Y and Kimura K. Bone morphogenetic protein 4 provides cancer-supportive phenotypes to liver fibroblasts in patients with hepatocellular carcinoma. J Gastroenterol 2019; 54: 1007-1018.

[54] Zhang L, Sun H, Zhao F, Lu P, Ge C, Li H, Hou H, Yan M, Chen T and Jiang G. BMP4 adminis-

tration induces differentiation of CD133+ hepatic cancer stem cells, blocking their contributions to hepatocellular carcinoma. Cancer Res 2012; 72: 4276-4285.

[55] Qian SW, Tang Y, Li X, Liu Y, Zhang YY, Huang HY, Xue RD, Yu HY, Guo L, Gao HD, Liu Y, Sun X, Li YM, Jia WP and Tang QQ. BMP4-mediated brown fat-like changes in white adipose tissue alter glucose and energy homeostasis. Proc Natl Acad Sci U S A 2013; 110: E798-807.

[56] Schornack PA and Gillies RJ. Contributions of cell metabolism and H+ diffusion to the acidic pH of tumors. Neoplasia 2003; 5: 135-145.

[57] Atai NA, Renkema-Mills NA, Bosman J, Schmidt N, Rijkeboer D, Tigchelaar W, Bosch KS, Troost D, Jonker A and Bleeker FE. Differential activity of NADPH-producing dehydrogenases renders rodents unsuitable models to study IDH1R132 mutation effects in human glioblastoma. J Histochem Cytochem 2011; 59: 489-503.

[58] Chang CJ, Mulholland DJ, Valamehr B, Mossessian S, Sellers WR and Wu H. PTEN nuclear localization is regulated by oxidative stress and mediates p53-dependent tumor suppression. Mol Cell Biol 2008; 28: 3281-3289.

[59] Hosako M, Ogino T and Okada S. Cell cycle arrest by physiological oxidant through the oxidation of retinoblastoma protein. Cell Struct Funct 2005; 30: 29-29.

[60] Maddocks OD, Berkers CR, Mason SM, Zheng L, Blyth K, Gottlieb E and Vousden KH. Serine starvation induces stress and p53-dependent metabolic remodelling in cancer cells. Nature 2013; 493: 542-546.

[61] K CS, Cárcamo JM and Golde DW. Antioxidants prevent oxidative DNA damage and cellular transformation elicited by the over-expression of c-MYC. Mutat Res 2006; 593: 64-79.

[62] Bell HS and Ryan KM. Intracellular signalling and cancer: complex pathways lead to multiple targets. Eur J Cancer 2005; 41: 206-215.

[63] Yasuda S, Arii S, Mori A, Isobe N and Imamura M. Hexokinase II and VEGF expression in liver tumors: correlation with hypoxia-inducible factor 1 alpha and its significance. J Hepatol 2004; 40: 117-123.

[64] Dewaal D, Nogueira V, Terry AR, Patra KC, Jeon SM, Guzman G, Au J, Long CP, Antoniewicz MR and Hay N. Hexokinase-2 depletion inhibits glycolysis and induces oxidative phosphorylation in hepatocellular carcinoma and sensitizes to metformin. Nat Commun 2018; 9: 2539.

[65] Dai W, Wang F, Lu J, Xia Y and Guo C. By reducing hexokinase 2, resveratrol induces apoptosis in HCC cells addicted to aerobic glycolysis and inhibits tumor growth in mice. Oncotarget 2015; 6: 13703-13717.

[66] Zhao R, Li L, Yang J, Niu Q, Wang H, Qin X, Zhu N and Shi A. Overexpression of pyruvate kinase M2 in tumor tissues is associated with poor prognosis in patients with hepatocellular carcinoma. Pathol Oncol Res 2020; 26: 853-860.

[67] Li S, Wu L, Feng J, Li J, Liu T, Zhang R, Xu S, Cheng K, Zhou Y and Zhou S. In vitro and in vivo study of epigallocatechin-3-gallate-induced apoptosis in aerobic glycolytic hepatocellular carcinoma cells involving inhibition of phosphofructokinase activity. Sci Rep 2016; 6: 28479.

[68] Wang RN, Green J, Wang Z, Deng Y, Qiao M, Peabody M, Zhang Q, Ye J, Yan Z, Denduluri S, Idowu O, Li M, Shen C, Hu A, Haydon RC, Kang R, Mok J, Lee MJ, Luu HL and Shi LL. Bone Morphogenetic Protein (BMP) signaling in development and human diseases. Genes Dis 2014; 1: 87-105.

[69] Bragdon B, Moseychuk O, Saldanha S, King D, Julian J and Nohe A. Bone morphogenetic proteins: a critical review. Cell Signal 2011; 23: 609-620.

Table S1. BMP4 IHC score criteria and outcomes

Degree	BMP4	Score			
Blue	Negative	0			
Light yellow	Weakly positive	1			
Brownish yellow	Moderately positive	2			
Dark brown	Strongly positive	3			

Range	BMP4	Score			
< 5% positive cells	Negative	0			
< 25% positive cells	Weakly positive	1			
< 50% positive cells	Moderately positive	2			
> 75% positive cells	Strongly positive	3			

BMP4 IHC score	HCC			Paracancer		
Specimen number	Degree	Range	Degree+Range	Degree	Range	Degree+Range
No.1	3	2	5	0	0	0
No.2	0	0	0	2	2	4
No.3	3	2	5	1	2	3
No.4	0	0	0	0	0	0
No.5	1	2	3	0	0	0
No.6	3	3	6	1	1	2
No.7	2	1	3	0	0	0
No.8	2	1	3	0	0	0
No.9	3	3	6	2	1	3
No.10	3	2	5	2	1	3
No.11	1	2	3	3	3	6
No.12	1	3	4	3	3	6
No.13	1	2	3	1	1	2
No.14	3	1	4	0	0	0
No.15	3	2	5	1	1	2
No.16	1	1	2	1	1	2
No.17	3	2	5	1	1	2
No.18	1	1	2	2	2	4
No.19	3	2	5	1	1	2
No.20	2	2	4	1	1	2
No.21	1	2	3	3	1	4
No.22	1	1	2	1	1	2
No.23	1	1	2	3	2	5
No.24	1	2	3	2	2	4
No.25	3	2	5	3	2	5
No.26	3	3	6	1	2	3
No.27	2	3	5	1	3	4
No.28	2	3	5	1	3	4
No.29	1	2	3	3	2	5
No.30	1	3	4	0	0	0
No.31	1	2	3	0	0	0
No.32	1	1	2	0	0	0
No.33	2	1	3	0	0	0
No.34	1	2	3	0	0	0
No.35	1	2	3	1	1	2
No.36	3	2	5	0	0	0

No.37	1	3	4	0	0	0
No.38	1	3	4	0	0	0
No.39	3	3	6	0	0	0
No.40	1	1	2	3	1	4

The standard of Anti-BMP4 IHC score.

Table S2. List of siRNA oligos

Gene	siRNA sequence	Accession No.
Human BMP4 siRNA-1	TTATTCTTCTTCCTGGCCC	NM_001202.6
Human BMP4 siRNA-2	TTCTCCAGATGTTCTTCGT	
Human BMP4 siRNA-3	ATACTCAAGACCAGTGCTG	

Table S3. List of TqPCR primers

Gene	Forward primer	Reverse primer	Accession No.
human Gapdh	ACCCAGAAGACTGTGGATGG	CACATTGGGGGTAGGAACAC	NM_008084
human Hk4	CGTCATCAACCGCATGCG	GGCATGGAACCGCTCCTT	NM_000162.5
human Hk2	CGAGGCCGCATCTCAGAG	TGTTGCAGGATGGCTCGG	NM_000189.5
human Pfkl	TAACTGTGCTGGGCCACG	AGCCGCACTGACTGGTTC	NM_001002021.3
human Pfkm	TTGGGGCATGTGCAGAGG	CGCACAGCCTGGTTACCA	NM_000289.6
human Pkl/r	TTGCTGTCACCCGCTCTG	AACACGGAGGAAGCCACG	NM_000298.6
human Pkm1/2	TGCAACCGAGCTGGGAAG	CCAGGACTGCATTGGCCA	NM_001206796.3
human Smad1	TGTGTCACCATTCCCCGC	GGCTCTGAAGATCGGGCC	NM_001003688.1
human Smad5	AGCAGCTGCAGCCTCAAA	CCAACATGGGGTGCTGGT	NM_001001419.3
human Smad8	CCTGTGCTCGTGCCAAGA	CACGGAGGCTGCTGGAAA	NM_001127217.3
human Smad6	GGAGCTGAAGCCCCTGTG	AGGGAGGTGGCGGAGATT	NM_005585.5
human Smad7	CGAGAGTGGGGAGGCTCT	CAGCCGATTTTGCTCCGC	NM_001190821.1

2

BMP4 protects HCC cells by glucose metabolic reprogramming

Figure S1. A. The determination of the optimal concentration of $CoCl_2$ for chemically induced hypoxia. 100 μM, 1 mM and 10 mM $CoCl_2$ were used to treat the Hu7 and MHCC97H cells for 72 h, and the cellular morphology was been observed under a bright field microscope (×100). B. The use of Ad-B4 and Ad-siB4 to infect Hu7 and MHCC97H cells. The Hu7 and MHCC97H cells were infected with Ad-B4, Ad-siB4, Ad-GFP or Ad-RFP. The fluorescence was observed under a fluorescence microscope at 48 h after infection (×100). C. Verification of the efficiency of Ad-B4 or Ad-siB4 in the Hu7 and MHCC97H cells. The Hu7 and MHCC97H cells were infected with Ad-B4, Ad-siB4, Ad-GFP or Ad-RFP for 48 h and TqPCR was used to analysis the expression of *Bmp4*. "**" $P < 0.01$, "*" $P < 0.05$, Ad-B4 group vs. Ad-GFP group, Ad-siB4 group vs. Ad-RFP group. D. The elevated expression of HK2, PFKFB3 and PKM2 in HCC tumor tissues. Paired liver tumor tissue (T) and adjacent liver non-tumor tissue (ALNT) samples from BMP4 high expression patients were evaluated by IHC staining. The expression of HK2, PFKFB3 and PKM2 was observed under a bright field microscope (×400). Positive stainings were indicated by arrows. Representative results were shown.
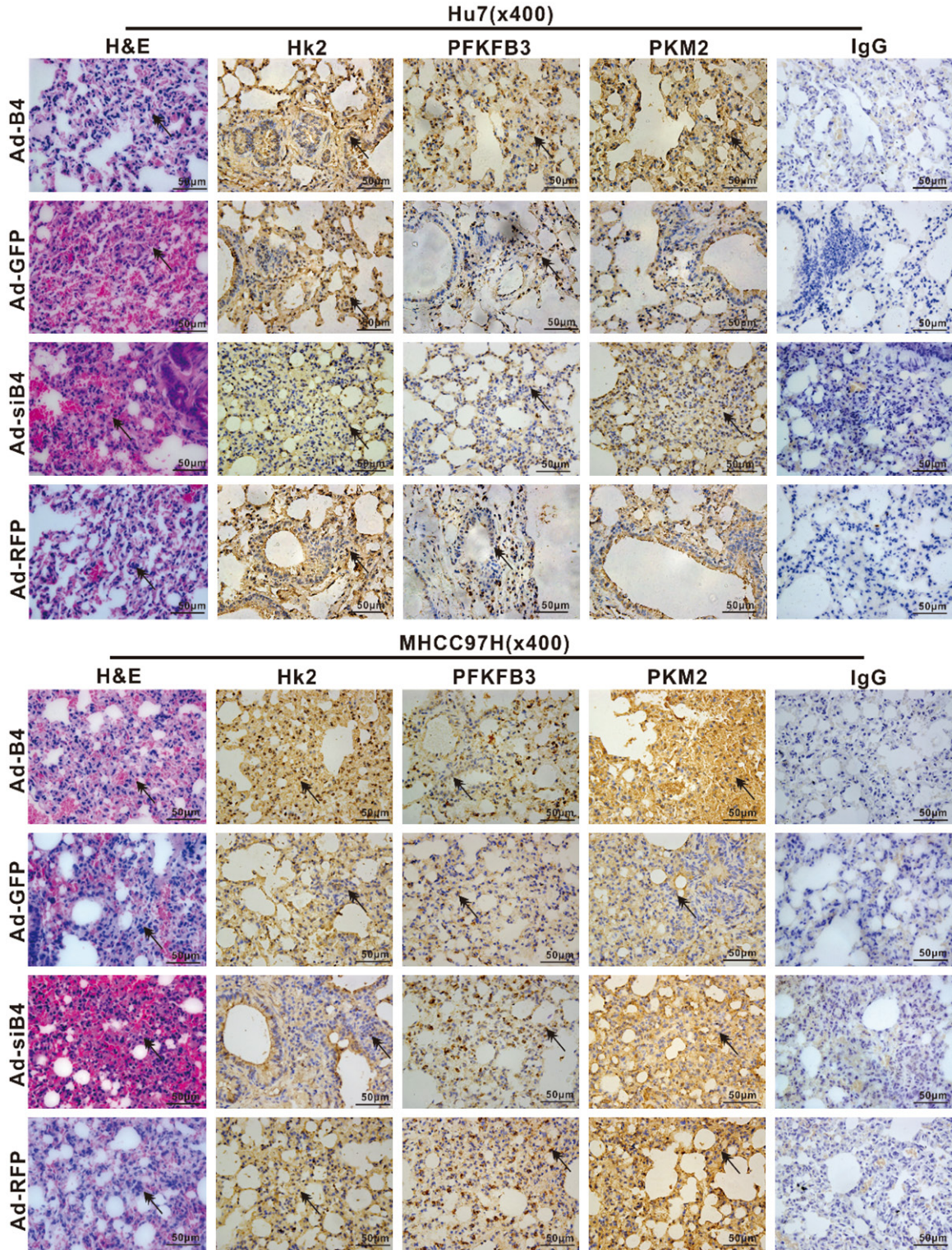
Figure S2. The elevated expression of HK2, PFKFB3 and PKM2 in the lung metastases of HCC cells *in vivo*. The retrieved mouse lung tissues were subjected to H & E and IHC staining, the morphological changes and expression of HK2, PFKFB3 and PKM2 were observed under a bright field microscope (×400). The typical metastases were indicated by arrows in H & E staining, and positive stainings of HK2, PFKFB3 and PKM2 were indicated by arrows in IHC staining. Representative results were shown.
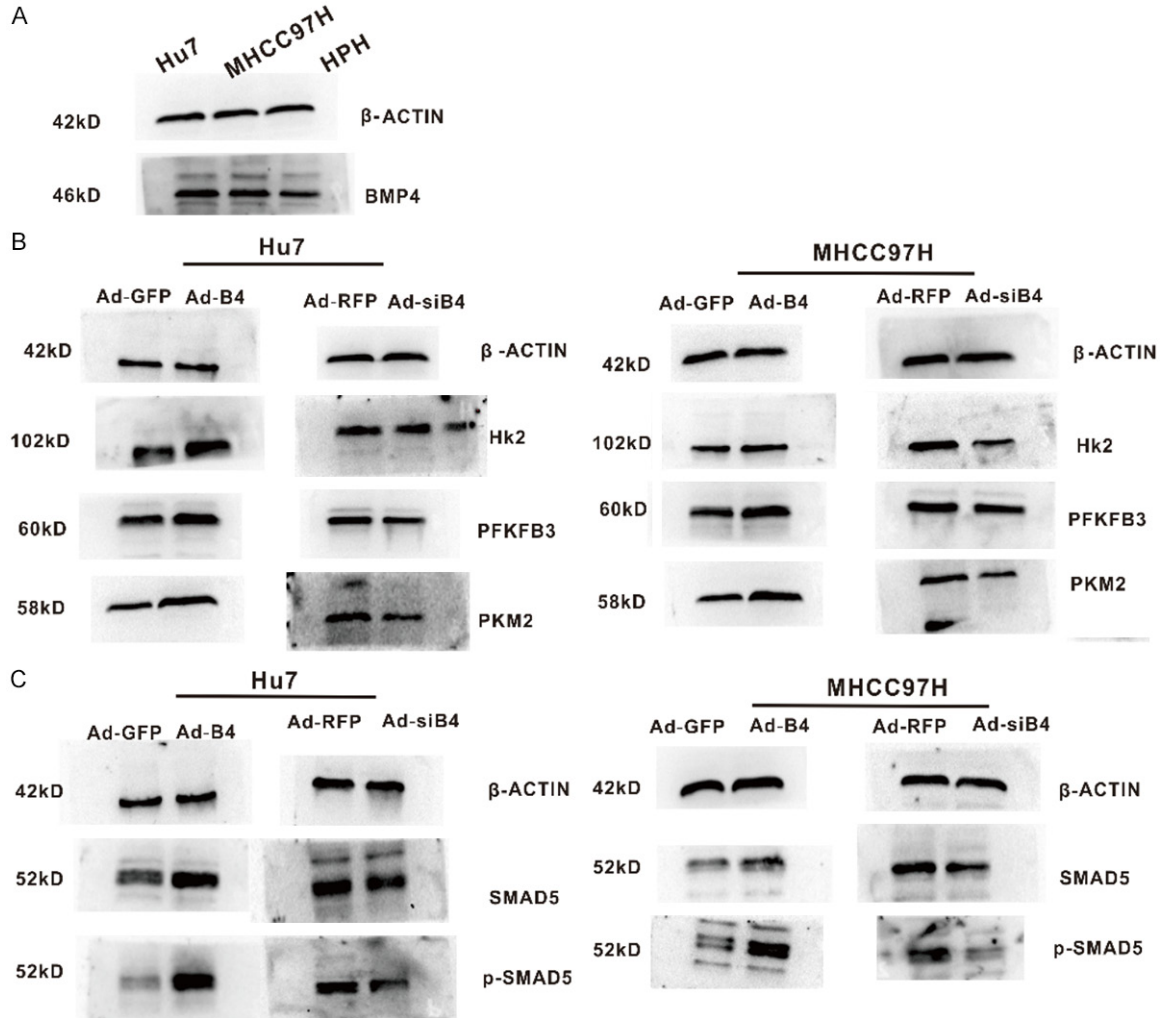
Figure S3. The original, full-length blot images shown in **Figures 1**, **4** and **5**.

Table S4. List of PCR primers for ChIP assay

Seqeunce	Forward primer	Reverse primer
PCR Frag-1 of HK2	ACCCAGAAGACTGTGGATGG	CACATTGGGGGTAGGAACAC
PCR Frag-2 of HK2	CGTCATCAACCGCATGCG	GGCATGGAACCGCTCCTT
PCR Frag-3 of HK2	CGAGGCCGCATCTCAGAG	TGTTGCAGGATGGCTCGG
PCR Frag-1 of PFKM	TAACTGTGCTGGGCCACG	AGCCGCACTGACTGGTTC
PCR Frag-2 of PFKM	TTGGGGCATGTGCAGAGG	CGCACAGCCTGGTTACCA
PCR Frag-3 of PFKM	TTGCTGTCACCCGCTCTG	AACACGGAGGAAGCCACG
PCR Frag-1 of PKM	TGCAACCGAGCTGGGAAG	CCAGGACTGCATTGGCCA
PCR Frag-2 of PKM	TGTGTCACCATTCCCCGC	GGCTCTGAAGATCGGGCC
PCR Frag-3 of PKM	AGCAGCTGCAGCCTCAAA	CCAACATGGGGTGCTGGT